


Cytopathology of Bronchoalveolar Lavages in COVID-19 Pneumonia: A Pilot Study

Valentina Canini, MD¹; Francesca Bono, MD¹; Paolo Calzavacca, MD²; Giulia Capitoli, PhD³; Giuseppe Foti, MD²; Filippo Fraggetta, MD⁴; Stefania Galimberti, PhD³; Andrea Gianatti, MD⁵; Marco Giani, MD²; Ahmed Nasr, MD¹; Giuseppe Paciocco, MD⁶; Fabio Pagni, MD ¹; Roberto Rona, MD²; and Vincenzo L'Imperio, MD¹

BACKGROUND: Bronchoalveolar lavage (BAL) in patients with severe coronavirus disease 2019 (COVID-19) may provide additional and complementary findings for the management of these patients admitted to intensive care units (ICUs). This study addresses the cytological features of the infection and highlights the more influential inflammatory components. The correlation between pathological variables and clinical data is also analyzed. **METHODS:** The authors performed a retrospective analysis of the cytopathological features of BAL in 20 COVID-19 patients and 20 members of a matched cohort from a critical ICU who had acute respiratory distress syndrome caused by other pulmonary conditions. **RESULTS:** A comparison of the controls (n = 20) and the COVID-19 patients (n = 20) revealed that the latter had a higher neutrophil count (median, 63.8% of the cell count) with lower percentages of macrophages and lymphocytes. An increase in the expression of CD68-positive, monocytic multinucleated giant cells (MGCs) was reported; megakaryocytes were not detected on CD61 staining. Perls staining showed isolated elements. In situ RNA analysis demonstrated scattered chromogenic signals in type II pneumocytes. An ultrastructural analysis confirmed the presence of intracytoplasmic vacuoles containing rounded structures measuring 140 nm in diameter (putative viral particles). In COVID-19 patients, the clinicopathological correlation revealed a positive correlation between lactate dehydrogenase values and MGCs ($r = 0.54$). **CONCLUSIONS:** The analysis of BAL samples might be implemented as a routine practice for the evaluation of COVID-19 patients in ICUs in the appropriate clinical scenario. Additional studies using a larger sample size of patients who developed COVID-19 during the second wave of the epidemic in the autumn of 2020 are needed to further support our findings. *Cancer Cytopathol* 2021;129:632-641. © 2021 American Cancer Society.

KEY WORDS: bronchoalveolar lavage (BAL); coronavirus disease 2019 (COVID-19); multinucleated giant cell; severe acute respiratory syndrome coronavirus 2 (SARS-CoV-2).

INTRODUCTION

The traditional clinical diagnostic scenario of pathologists was disrupted by the advent of the new coronavirus disease 2019 (COVID-19) epidemic, which spread globally from January 2020.¹ The intrinsic emergency related to the viral epidemic provided urgent answers to pneumologists and intensive care unit (ICU)

Corresponding Author: Fabio Pagni, MD, Pathology, Department of Medicine and Surgery, Azienda Socio Sanitaria Territoriale di Monza, University of Milano-Bicocca, Via Cadore 48, 20900, Monza, Italy (). E-mail: fabio.pagni@unimib.it

¹Pathology, Department of Medicine and Surgery, Azienda Socio Sanitaria Territoriale di Monza, University of Milano-Bicocca, Monza, Italy; ²Emergency and Intensive Care, Department of Medicine and Surgery, Azienda Socio Sanitaria Territoriale di Monza, University of Milano-Bicocca, Monza, Italy; ³Bicocca Bioinformatics Biostatistics and Bioimaging B4 Center, School of Medicine and Surgery, University of Milano-Bicocca, Monza, Italy; ⁴Pathology, Cannizzaro Hospital, Catania, Italy; ⁵Azienda Socio Sanitaria Territoriale Papa Giovanni XXIII, Bergamo, Italy; ⁶Pneumology, Department of Medicine and Surgery, Azienda Socio Sanitaria Territoriale di Monza, University of Milano-Bicocca, Monza, Italy

All except the first and last authors are listed in alphabetical order.

This article is dedicated to the victims of the first peak of the severe acute respiratory syndrome coronavirus 2 epidemic in Northern Italy. In memory of Marco Giussani, we thank the technical staff that allowed the performance of this study through their specialized contributions, particularly Virginia Brambilla, Marina Covre, Elena Crocco, and Barbara Vergani.

Additional supporting information may be found in the online version of this article.

Received: November 25, 2020; **Revised:** February 11, 2021; **Accepted:** February 11, 2021

Published online March 10, 2021 in Wiley Online Library (wileyonlinelibrary.com)

DOI: 10.1002/cncy.22422, wileyonlinelibrary.com

specialists. In the past several months, the progressive increase in the histological knowledge of this infection, mainly from autopsies, prompted the establishment of diagnostic criteria.^{2,3} This entity showed various histopathological patterns, which ranged from early acute lung injury with interstitial pneumonitis to acute and/or organizing diffuse alveolar damage.⁴ Autopsies produced an organic overview of the COVID-19 landscape in the lungs; as a second step, pathologists are translating the histological information into mini-invasive samples such as bronchoalveolar lavage (BAL), which might play a significant role in the multidisciplinary workup of severe acute respiratory syndrome coronavirus 2 (SARS-CoV-2) infection by recognizing the predominant inflammatory cell populations and determining the correlation of cytopathology to the clinical parameters.^{5,6}

This pilot study was aimed at exploring the essential diagnostic cytological features of BAL samples from COVID-19 patients. This article approaches the issue by integrating traditional morphology with indispensable ancillary techniques such as RNAscope and transmission electron microscopy (TEM), which have made important contributions to the characterization of BAL samples.

MATERIAL AND METHODS

Study Design

We performed a retrospective, observational study including patients from 2 large tertiary hospitals (Azienda Socio Sanitaria Territoriale di Monza and Azienda Socio Sanitaria Territoriale Papa Giovanni XXIII, Bergamo, Italy) during the first peak of the pandemic. We analyzed the characteristics of BAL samples from 20 COVID-19 patients admitted to ICUs with a diagnosis of acute respiratory distress syndrome (ARDS) and from a matched group of 20 patients with ARDS caused by other etiologies (7 with interstitial lung disease, 7 with bacterial pneumonia, 2 with viral influenza pneumonia, 2 with fungal pneumonia, 1 with antineutrophil cytoplasmic antibody-associated vasculitis, and 1 with mycobacterial pneumonia). The patients included in the matched cohort were retrospectively enrolled from September 2019, far from the pandemic period. The COVID-19 cohort included patients who tested positive for SARS-CoV-2 on a real-time polymerase chain reaction analysis of nasal

swabs ($n = 15$; 3 were performed after BAL execution) and BAL samples ($n = 5$). Individual matching was performed with respect to patients' sex, age (± 5 years), need for invasive mechanical ventilation, and antibiotic therapy status (previous or current). COVID-19 patients and controls were stratified into 2 groups: patients with mild respiratory disease (ie, those requiring only oxygen supplementation) and patients with moderate to severe ARDS under invasive mechanical ventilation. This stratification was consistent with that used in large clinical trials⁷ and indicated in international guidelines.⁸ The study was conducted in accordance with the standards of Good Clinical Practice, the ethical principles of the Helsinki Declaration, and current legislation on observational studies. Data were gathered in the context of a larger prospective study on SARS-CoV2 patients approved by the local Ethics Committee (Ethical Board Monza e Brianza).

BAL Procedure

In nonintubated patients, the upper airway was injected with 4 mL of 2% lidocaine. An additional dose of lidocaine (1%) was administered to the lower airways after the introduction of a flexible fiberoptic bronchoscope to suppress coughing (1T10; Olympus, Tokyo, Japan). In intubated patients, a flexible bronchoscope was introduced via the endotracheal tube. Every ventilator circuit featured a closed suction system with a sealed valve side port (5.0 mm in size) for bronchoscopy. This system can be used during the entire intubation period (replaced every 72 hours) and may substantially reduce the risk of aerosolization during endotracheal suctioning or bronchoscopy.⁹ BAL was performed in the lung area with considerable abnormalities on high-resolution computed tomography. Consecutive 10-mL aliquots of a sterile saline solution, warmed at 37 °C, were infused (up to 100 mL). Fluid samples were gently aspirated immediately after each aliquot was introduced and were collected in a sterile container. Two or more satisfactory specimens were obtained from at least 2 segments. The protocol included passes from a single lobe in COVID-19 patients admitted to the ICU because of their critical conditions.

Clinical Data

Patients' clinical data were obtained: sex, date of birth, medical history (diabetes, hypertension, obesity, and smoking), death, laboratory tests (peripheral blood cell

count, lactate dehydrogenase [LDH] level, and D-dimer level), blood gas analysis results (arterial oxygen pressure [PaO_2] and arterial carbon dioxide pressure), oxygenation parameters (fraction of inspired oxygen [FiO_2] and $\text{PaO}_2/\text{FiO}_2$), antibiotic/antiviral therapies, length of stay (from date of hospitalization to ICU discharge or death), and timing of BAL execution (from the onset of symptoms to BAL execution, from nasal swab to BAL execution, from hospitalization to BAL execution, and from the introduction of invasive ventilation to discharge/death).

Cytopathology

Cytological samples collected from COVID-19 patients were processed according to the proposed guidelines,¹⁰ and all the procedures were conducted by an experienced cytotechnician using appropriate personal protective equipment (masks, gloves, and a face shield) in a class II biosafety cabinet, as recommended.¹¹ Upon arrival at the pathology department, fresh pulmonary samples were fixed with 70% alcohol and 10% neutral buffered formalin for 12 hours. An aliquot of every sample was centrifuged (Labofuge AE, Heraeus, Germany) at 800 rpm for 10 minutes at +4 °C, and the obtained cell pellet was washed twice with phosphate-buffered saline (without Ca^{++} and Mg^{++}). The obtained cytocentrifugates were then stained with both May-Grünwald-Giemsa and Papanicolaou stains. From the formalin-fixed aliquot, cell blocks were prepared as previously described.¹² Diagnostic cytocentrifugation (cytospin) and hematoxylin-eosin-stained sections were examined by a joint panel of lung pathologists (F.P., F.B., and F.F.). The differential cell count (lymphocytes, neutrophils, eosinophils, mast cells, plasma cells, macrophages, and multinucleated giant cells [MGCs]) was determined with the May-Grünwald-Giemsa-stained cytospin after the assessment of 200 cells at $\times 400$ magnification in random fields; pure numbers were recorded and then turned into percentages based on the total number of cells counted. A section of the cell block was stained with Perls (Prussian blue) to evaluate the presence of iron-laden macrophages. Hematoxylin-eosin staining was used to confirm the morphology of cells.

Immunocytochemistry, RNAscope, and TEM

Immunocytochemistry (ICC) analyses were performed with the Omnis platform (Dako, Glostrup, Denmark). The immunostains used included pancytokeratin (AE1/AE3; Dako), TTF1 (8G7G3/1), CD20 (L26), CD3

(polyclonal), CD4 (4B12), CD8 (C8/144B), CD68 (PGM1), and CD61 (Y2/51). RNAscope (RNAscope 2.5 LS Probe V-nCoV2019-S, #848568, and RNAscope 2.5 LS Reagent Kit-RED, #322150; Advanced Cell Diagnostics) was performed on formalin-fixed, paraffin-embedded cell blocks on a Leica BOND RX multiplex stainer. The quality of the tissue was tested with the messenger RNA of the PPIB housekeeping gene, which has constitutive expression in different tissues. Additional specimens were centrifuged, extracted from the preservation alcoholic solution, and fixed in 4% buffered glutaraldehyde with 0.2 M sodium cacodylate for TEM. After fixation, the cytological material was coagulated in 1.5% gelose, embedded in EPON resin, and processed as previously described to obtain thin sections.¹³

Statistical Analysis

Categorical data were expressed as frequencies and percentages, whereas continuous data were expressed as measures of location (ie, means and medians) and variability (ie, standard deviations and quartiles I-III), as appropriate. The direction and strength of the linear association between 2 quantitative variables were quantified with the Pearson correlation coefficient. The between-group comparisons of quantitative, categorical, and time-to-event variables were performed with the Mann-Whitney test, the χ^2 test (or the Fisher test), and the log-rank test, respectively. The Benjamini and Hochberg method was applied to adjust for multiplicity, and the *P* values were reported in their adjusted version. The tests were 2-sided and had a significance level of .05. All statistical analyses were performed with open-source R software (version 3.6.0).

RESULTS

Twenty COVID-19 patients and 20 matched controls were included in the study. The 2 groups were similar in terms of age, sex, antiviral/antibiotic therapy, and comorbidities (Table 1). In the COVID-19 and control cohorts, the most common comorbidities were hypertension and diabetes, but only a few patients were obese or had a history of smoking. Among COVID-19 patients who underwent BAL to rule out concurrent pneumonia from other etiologies, only a minority ($n = 4$) showed the presence of a superimposed bacterial infection. No significant differences were observed in the laboratory tests performed at the time of BAL execution, as described in Table 2. According to the timing of BAL execution for

TABLE 1. Demographic and Clinical Characteristics at Diagnosis of Each Group

Characteristic	COVID-19 (n = 20)	Controls (n = 20)	P
Demographics			
Age, mean (SD), y	63 (11)	67 (10)	.2334
Sex: female, No. (%)	8 (40)	8 (40)	
Clinical, No. (%)			
Hypertension	10 (50)	8 (40)	.7506
Diabetes	6 (30)	6 (30)	1
Smoke	1 (5)	4 (20)	.3390
Obesity	2 (10)	3 (15)	1
Antibiotic/antiviral ^a	19 (95)	19 (95)	1
Death, No. (%)	3 (15)	7 (35)	
Nasal swab for SARS-CoV-2 detection, No. (%)	15 (75)	—	
BAL for SARS-Cov-2 detection, No. (%)	5 (25)	—	
Reasons for BAL performance, No.			
Suspected bacterial infection	5	7	
Suspected viral infection	3	2	
Suspected fungal infection	3	2	
SARS-CoV-2 infection	5	—	
Other	4 ^b	9 ^c	
Superimposed infections, No.	4	—	

Abbreviations: BAL, bronchoalveolar lavage; COVID-19, coronavirus disease 2019; SARS-CoV-2, severe acute respiratory syndrome coronavirus 2; SD, standard deviation.

^aAlready performed or in progress at the time of the BAL procedure.

^bAlveolar hemorrhage was excluded in 2, lymphoma was excluded in 1, and lung cancer was excluded in 1.

^cSeven had suspected interstitial lung disease, 1 had mycobacterial pneumonia, and 1 had antineutrophil cytoplasmic antibody-associated vasculitis.

both cohorts and the relative subgroups (mild vs moderate to severe), only hospital length of stay showed a significant difference: it was shorter for COVID-19 patients with mild respiratory disease versus moderate to severe respiratory disease (median, 24 vs 51 days; $P = .007$). The other periods considered (from the onset of symptoms to BAL execution, from the nasal swab to BAL execution, from the hospitalization to BAL execution, and from the introduction of invasive ventilation to discharge/death) failed to show any relevant differences among the groups (Supporting Table 1).

Cytopathology

The cytopathology parameters are summarized in Table 3. COVID-19 patients exhibited higher neutrophil counts (median, 63.8% [quartiles I-III, 32.0%-68.9%] vs 10.8% [quartiles I-III, 5.7%-37.9%]; $P = .0097$) and lower percentages of macrophages (median, 25.5% [quartiles I-III, 11.3%-41.4%] vs 73.7% [quartiles I-III, 46.8%-84.7%]; $P = .0022$), as shown in Figure 1. They also showed higher

expression of MGCs (median, 0.37% [quartiles I-III, 0%-1.52%] vs 0% [quartiles I-III, 0%-0%]; $P = .0562$), although the comparison was borderline significant. The analysis of the dynamic changes in the inflammatory composition of BAL samples from COVID-19 patients showed a strong negative correlation between neutrophils and macrophages ($r = -0.77$; $P = .0001$) and a mild negative correlation between neutrophils and lymphocytes ($r = -0.47$; $P = .0385$). This comparison showed a similar but weaker trend in the matched non-COVID-19 controls ($r = -0.30$; $P = .2051$).

ICC, RNAscope, and TEM

T lymphocytes (CD3+) maintained a normal CD4/CD8 ratio, with only rare cases showing a slight prevalence of cytotoxic subsets. Being positive for CD68-pgm1, MGCs exhibited a monocytic origin (Fig. 2A); megakaryocytes were not detected on CD61 staining. Rare cases showed focal morphological atypia of lymphocytes, with isolated elements characterized by convoluted/cerebriform nuclei (Fig. 2B, top panel) corresponding to nuclear membrane irregularities and invagination in TEM (Fig. 2B, bottom panel). Perls staining showed isolated elements or small groups of iron-laden macrophages, which accounted for less than 10% of the cell count. Epithelial cells, both bronchial cells (cytokeratin AE1/AE3+/TTF1-) and pneumocytes (cytokeratin AE1/AE3+/TTF1+), were found in the majority of these specimens, some of which showed nuclear clearing, although real virally induced inclusions were not found in this series (Fig. 2C,D). In situ RNA analysis of cell blocks showed scattered chromogenic signals in type II pneumocytes (Fig. 2E). RNAscope-positive type II pneumocytes, evaluated by TEM (Fig. 2F), showed intracytoplasmic vacuoles containing rounded structures measuring 140 nm in diameter with an electron-dense layer on the inner side of the membrane; they possibly represented the nucleocapsid protein of these viral-like particles (Fig. 2G).

Clinical-Pathological Correlation

A significant and moderate positive correlation was observed between the LDH values and MGCs in the COVID-19 cohort ($r = 0.54$; $P = .0301$), with evidence of an even stronger correlation in the subgroup with moderate/severe cases ($r = 0.75$; $P = .0340$). The same analyses conducted in the control group did not show any correlation ($r = -0.19$; $P = .5544$). The remaining comparisons between clinical and cytological features

TABLE 2. Laboratory Data by Group at Bronchoalveolar Lavage Evaluation

Laboratory Characteristic	COVID-19			Controls		
	No.	Median	Quartiles I-III	No.	Median	Quartiles I-III
Pao ₂	17	80	71.10-99.90	19	88.60	64.90-101.45
Paco ₂	17	49	37.80-54.00	19	38.00	36.00-47.30
P/F	14	175	129.75-299.50	19	234.00	147.00-304.50
WBCs, 10 ³ /μL	20	10.4	7.02-15.23	20	8.48	4.53-10.67
Lymphocytes, %	18	14.1	11.93-21.00	20	12.45	8.12-18.72
Platelets, 10 ³ /μL	20	195	148.00-327.50	20	200.00	152.50-295.75
Lactate dehydrogenase, U/L	16	324	266.75-444.75	12	286.50	238.00-328.75
D-dimer, ng/mL	15	950	350.00-1838.00	13	1182.00	626.00-1811.00

Abbreviations: COVID-19, coronavirus disease 2019; Paco₂, arterial carbon dioxide pressure; Pao₂, arterial oxygen pressure; P/F, ratio of arterial oxygen pressure to fraction of inspired oxygen; WBC, white blood cell. Normal laboratory ranges were as follows: WBCs, 4.00 to 11.00 10³/μL; lymphocytes, 16.0% to 46.0%; platelets, 140.00 to 440.00 10³/μL; lactate dehydrogenase, 135 to 225 U/L; and D-dimer, 0 to 25 ng/mL.

TABLE 3. Cytological Characteristics Reported as Percentages of Inflammatory Cell Composition by Group

Cytological Characteristic	COVID (n = 20)		No COVID (n = 20)		P
	Median	Quartiles I-III	Median	Quartiles I-III	
Perls, %	4.0	0-18.5	0	0-2.75	.1873
Neutrophils, %	63.8	31.98-68.88	10.8	5.71-37.87	.0097
Eosinophils, %	0.0	0.00-0.22	0	0.00-1.34	.1873
Lymphocytes, %	8.7	5.65-15.01	3.7	1.94-12.11	.1873
Macrophages, %	25.5	11.29-41.38	73.7	46.81-84.72	.0022
Plasma cells, %	0.0	0.00-1.33	0	0-0	.1873
Multinucleated giant cells, %	0.4	0-1.52	0	0-0	.0562

Abbreviation: COVID-19, coronavirus disease 2019.

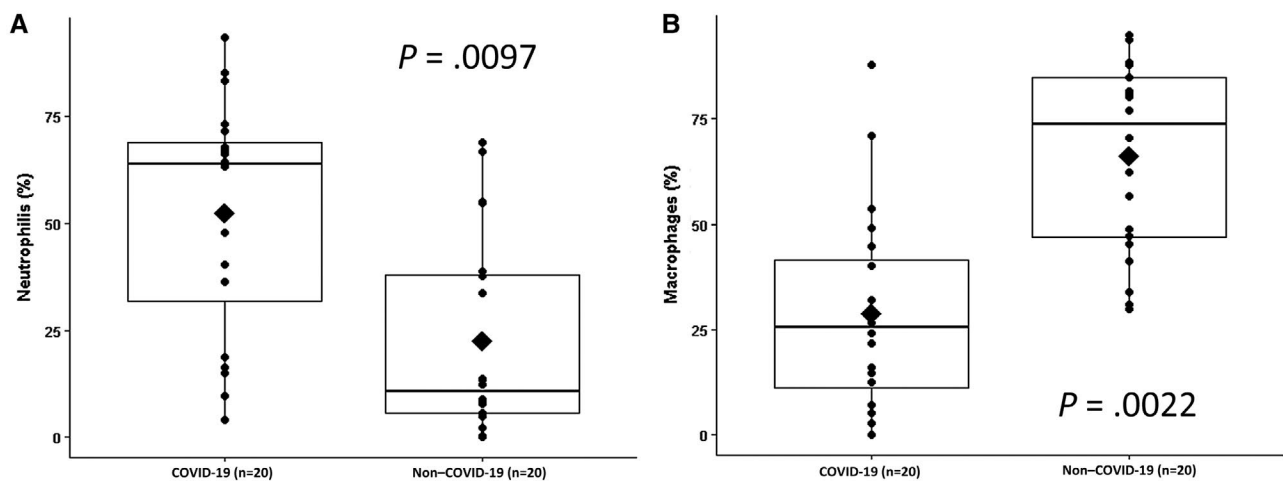


Figure 1. Box plots showing (A) the higher prevalence of neutrophils in the COVID-19 group and (B) the reverse prevalence of macrophages in the non-COVID-19 group. COVID-19 indicates coronavirus disease 2019.

of the cohorts revealed mainly weak correlations/trends (eg, between D-dimer and neutrophils or lymphocytes), although none of these comparisons showed significance. No trend was found between the Pao₂/Fio₂ ratio and the cytological parameters measured in BAL samples. The comparisons of respiratory and laboratory

variables among groups and subgroups failed to show significant differences (Supporting Table 2).

DISCUSSION

BAL in patients with severe COVID-19 disease may provide additional and complementary findings and might

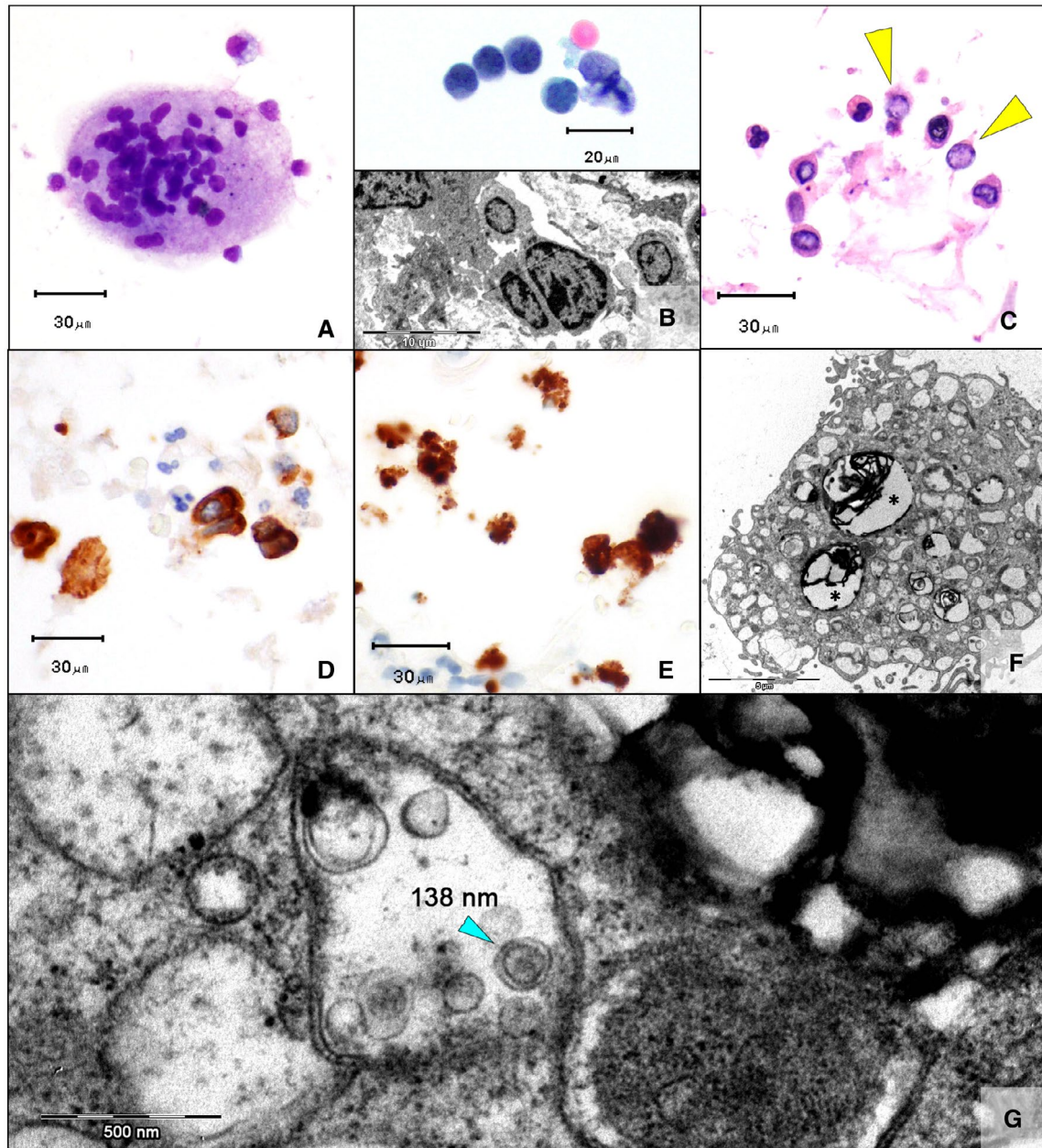


Figure 2. (A) Occasional multinucleated giant cells in COVID-19 patients (May-Grünwald-Giemsa, $\times 40$). (B) In some cases, lymphocytes showed nuclei with irregular contours, rarely with a cerebriform appearance (*Top*; Papanicolaou, $\times 60$), corresponding to the membrane invagination/convolution on electron microscopy (*Bottom*; $\times 1450$). (C) Type II pneumocytes with nuclear clearing and pseudo-inclusions (yellow arrowheads; H & E, cell block, $\times 40$). (D) These cells were positive for cytokeratin AE1/AE3 ($\times 40$), and (E) some were positive on RNAscope ($\times 40$). (F) Transmission electron microscopy confirmed the presence of intracytoplasmic lamellar bodies, which corresponded to the surfactant protein produced by type II pneumocytes (asterisks; $\times 4600$). (G) Intracytoplasmic vacuoles contained rounded structures measuring 140 nm in diameter with an electron-dense layer in the inner side of the membrane, which could correspond to the nucleocapsid protein of these viral-like particles ($\times 34,000$). COVID-19 indicates coronavirus disease 2019

play a significant role in the multidisciplinary workup of SARS-CoV-2 infection in ICUs by recognizing the predominant inflammatory cell populations and determining the correlation of cytopathology with the clinical parameters. High-resolution computed tomography

can noninvasively identify the specific imaging patterns strongly suggestive of COVID-19–related pneumonia. However, BAL in ICUs could further support this diagnosis and add the following information to the peripheral blood tests:

- Presence/absence of a secondary/superimposed infection. In this field, BAL is able to characterize the viral cytopathic effects and fungal pneumonia (by optional special stains).
- Presence of a significant hemorrhagic component by Perls staining.
- Co-occurrence of neoplastic bystander diseases (lymphoproliferative processes possibly related to the immune status of the patients).
- Putative COVID-19–related cytopathological signs (eg, MGCs).
- Relative percentages of the leukocytes in BAL samples. A trend in the results can help ICU clinicians in making and modulating therapeutic decisions.

No controlled clinical trials have evaluated whether routine BAL improves the final outcomes. Nevertheless, cytopathological analysis, staining for mycobacterial and fungal infections, and Perls staining may provide support or help to narrow the differential diagnosis. Systematic literature data have demonstrated the difficulty in weighing benefits against the risks and costs of the procedure.¹⁴ For this reason, the decision is usually determined on a case-by-case basis. Because of the intrinsic emergency related to the epidemic, BAL was routinely introduced in many ICUs in parallel with other diagnostic tools. Its usefulness is further reinforced by the use of technical preparations such as cell blocks that may be tested with ICC, in situ hybridization, DNA/RNA extraction, or TEM. Only the integration of morphology and additional techniques can lead to a final pathobiological understanding of the infection. The first diagnostic step is the recognition of the predominant inflammatory cell count (at least 200 cells per sample). Measuring the concentration of these cells may provide insights into the different stages of the disease and allow hypothesizing about the extent and quality of the tissue damage mini-invasively.¹⁵ This is a dynamic process that recalls the clinical progression observed in ICU patients (Fig. 3). The early negative correlation between neutrophils, lymphocytes, and macrophages is similar to that of other interstitial lung diseases, in which pronounced neutrophilia in BAL samples is generally associated with ARDS and acute interstitial pneumonia.^{16,17} The late phases of diffuse alveolar damage (DAD) are usually marked by lymphocytes and eosinophils to the point that the persistence of a high number of neutrophils may be associated with an unfavorable

prognosis.¹⁸⁻²⁰ In this setting, recent autoptic COVID-19 reports have described subsets of patients with increased numbers of intra-alveolar neutrophils in the absence of concurrent/superimposed bacterial lung infections, some of which show rapid progression and an aggressive clinical course.³ However, alterations in the inflammatory cell count in BAL samples, especially with an increase in the neutrophil count, should prompt an assessment for a concomitant bacterial/fungal infection. In the current study, patients with severe COVID-19 homogeneously showed BAL neutrophilia, although only a few patients ($n = 4$) in the whole group had a demonstrated concurrent bacterial infection. The putative role of neutrophils in the progression of COVID-19 disease has been postulated because of the evidence of neutrophil-derived extracellular traps, webs of chromatin, and microbicidal proteins that maintain the innate immune host defense, which may initiate and propagate inflammation and thrombosis.^{21,22} Uncontrolled immune thrombosis could induce collateral tissue damage and contribute to organ dysfunction with a loss of endothelial integrity and activation of platelets with production of vaso-occlusive thrombi in the pulmonary capillaries. In postmortem studies of COVID-19 patients, a notable megakaryocyte deposition was found in the pulmonary capillary vascular bed that accompanied DAD even in the exudative and proliferative phase. However, megakaryocytes were not noted, even with the performance of specific ICC (CD61). Further investigations in larger cohorts are needed to address the putative roles of different inflammatory components (eg, neutrophils) in the thrombotic states observed in patients with severe COVID-19 pneumonia. Although a hemorrhagic component may complicate the natural history of the disease, our results excluded the significant contribution of hemorrhagic alveolitis because Perls staining showed only scattered chromogenic signals in type II pneumocytes.²³ Conversely, the peculiar occasional detection of MGCs could be a sign of the progression toward late and more severe disease stages. CD68-positive MGCs can function as antigen-presenting cells or activated macrophages; they can represent highly stimulated monocytes at the terminal stage of maturation, and this multinucleation culminates in cell death. The histological counterpart of this finding has been well described recently, with approximately 50% of autoptic COVID-19 cases characterized by at least focally MGC-infiltrated lungs, which are frequently associated with the late proliferative or early organizational

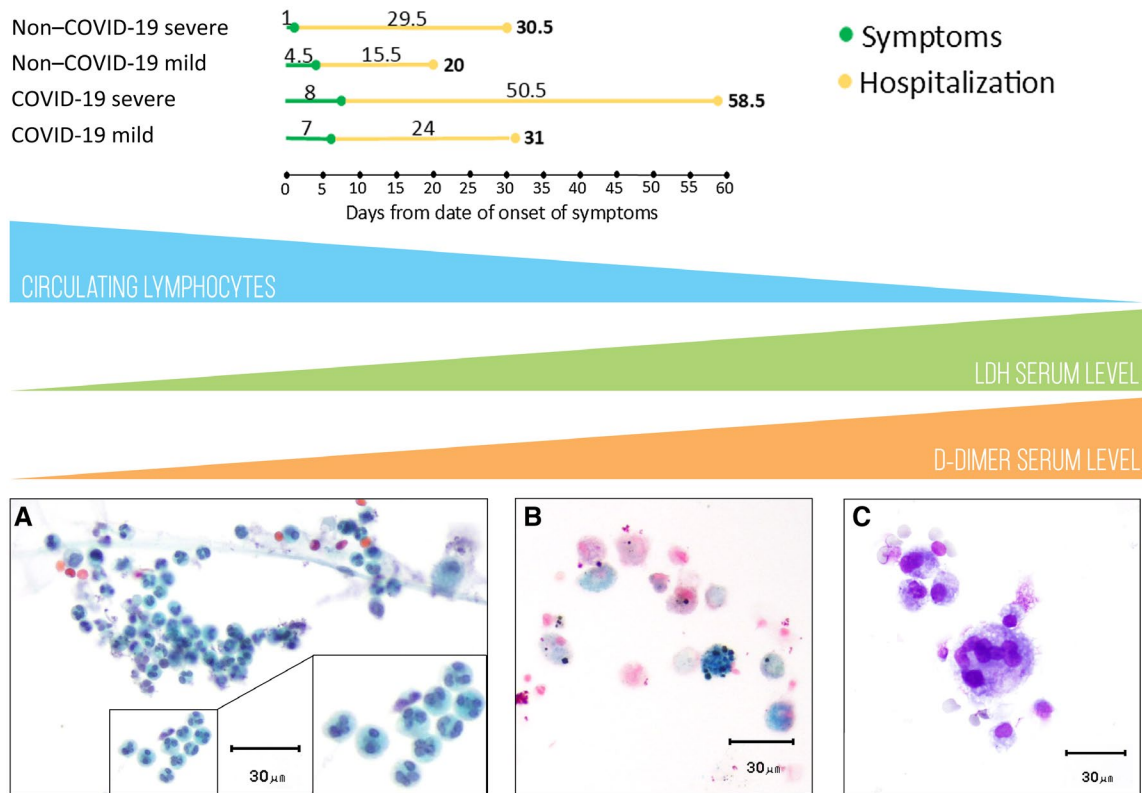


Figure 3. Possible correlation between SARS-CoV-2 infection and the clinical course from a BAL perspective. Patients from the COVID-19 and non-COVID-19 groups, divided into subgroups (those with severe cases and those with mild cases), had different lengths of stay. (A) The progressive lymphocytopenia and the increase in LDH/D-dimer were correlated with abscess-derived neutrophils in BAL samples (Papanicolaou, $\times 40$) (B) with a relative reduction in the number of macrophages, which were only rarely represented by Perl's-positive elements ($\times 40$). (C) Multinucleated giant cells were occasionally found (May-Grünwald-Giemsa, $\times 40$). BAL indicates bronchoalveolar lavage; COVID-19, coronavirus disease 2019; LDH, lactate dehydrogenase; SARS-CoV-2, severe acute respiratory syndrome coronavirus 2.

fibrotic phase of DAD, in which the lungs become extensively remodeled through the proliferation of dense myofibroblasts.^{24,25} Some authors have proposed that the formation of syncytial MGCs could represent a cytopathic effect induced by the virus, and they have even described the nuclear clearing of pneumocytes as a possible effect of a direct SARS-CoV-2 infection, the so-called covicyte.^{26,27} However, in light of the infection mechanism of this particular virus, which affects the cells expressing ACE2, the direct colonization of MGCs of macrophage origin is an unlikely event. Moreover, because the virus uses the cytoplasmic machinery for its replication without entering the nuclei of susceptible cells (eg, type II pneumocytes), the presence of classic nuclear virocytopathic changes is unexpected.²⁶ The absence of reliable morphological hints of direct viral infection to these epithelial elements (Fig. 2C) stresses the need for ancillary techniques, such as RNAscope (Fig. 2E) and TEM (Fig. 2F,G), to

investigate the presence of SARS-CoV-2. Many different ultrastructural descriptions of the virus have been reported in the literature in the last few months. However, a progressive understanding of its biology led to the accurate definition of the morphological criteria to define the true and reliable viral particles and helped to distinguish normally present intracytoplasmic vesicles such as multivesicular bodies and clathrin-coated vesicles.²⁸ In the setting of a COVID-19 infection, lymphocytes could show cytological abnormalities as well, as noted in peripheral blood.²⁹ These atypical morphological aspects generally range from plasmacytoid morphology with eccentric nuclei and intracytoplasmic halos⁵ to elements with large nuclei and evident nucleoli reminiscent of immunoblasts, whereas the Downey type II lymphocyte, generally associated with other viral infections, is less common. In the current study, rare cases showed small/intermediate-size lymphocytes with convoluted/cerebriform nuclei

(Fig. 2B, top panel), which corresponded to invaginated nuclear membranes, as shown on electron microscopy analysis (Fig. 2C, bottom panel). Whether these findings are specific for the SARS-CoV-2 infection is still under debate and requires further investigation.

The study of the clinical course of COVID-19 disease led to an understanding of the progressive modifications of laboratory parameters, which could potentially guide the management of these patients. The association of cytological findings with known progressive lymphopenia³⁰ and increases in LDH³¹ and D-dimer levels²¹ could further help ICU specialists and elucidate the pathogenetic relationships among inflammatory and biochemical phenomena. In this setting, the strong positive correlation between LDH values and MGCs ($r = 0.54$), especially in the severe subgroup ($r = 0.75$), possibly indicates a progressive proinflammatory process, as already demonstrated in mouse models, where the detection of MGCs in BAL samples was directly proportional to increased LDH as a marker of cellular damage.²²

In conclusion, BAL is a procedure aimed at obtaining cells from the airways that can provide important and quick information regarding the status of infections and interstitial lung diseases. The results of the cytological analysis should be applied in the appropriate clinical scenario, and it should be determined whether the findings of this analysis have a strong correlation with the imaging or laboratory data. The potential translatability of histological findings from autopsies to cytopathology is an important step for the routine management of COVID-19 patients in ICUs because invasive diagnostic procedures can be avoided. Because several histopathological studies have reported that DAD is the main injury pattern in lungs affected by SARS-CoV-2 infection, BAL is performed as a complementary dynamic confirmatory test. Larger studies including more patients with mild and moderate to severe cases from the second wave of the epidemic in the autumn of 2020 are needed to further support our findings and eventually highlight some cytological insights that can distinguish patients with a more aggressive course.

FUNDING SUPPORT

No specific funding was disclosed.

CONFLICT OF INTEREST DISCLOSURES

The authors made no disclosures.

AUTHOR CONTRIBUTIONS

Valentina Canini: Selection of the cases to be included in the study and management and coordination of the collection of both clinical and cytological data. **Francesca Bono:** Assessment of the cytological samples, performance of the inflammatory cell count for cases and controls, and interpretation of the immunocytochemical results. **Paolo Calzavacca:** Provision of the cohorts' clinical data as well as the gas exchange and therapy details for every patient. **Giulia Capitoli:** Statistical analysis. **Giuseppe Foti:** Provision of the cohorts' clinical data as well as the gas exchange and therapy details for every patient. **Filippo Frassetto:** Assessment of the cytological samples, performance of the inflammatory cell count for cases and controls, and interpretation of the immunocytochemical results. **Stefania Galimberti:** Statistical analysis. **Andrea Gianatti:** Provision of the cytological specimens from the Bergamo Center, performance of the RNAscope assay, and interpretation of the results. **Marco Giani:** Performance of the bronchoalveolar lavage procedure. **Ahmed Nasr:** Provision of the cytological specimens from the Bergamo Center, performance of the RNAscope assay, and interpretation of the results. **Giuseppe Paciocco:** Performance of the bronchoalveolar lavage procedure. **Fabio Pagni:** Assessment of the cytological samples, performance of the inflammatory cell count for cases and controls, and interpretation of the immunocytochemical results. **Roberto Rona:** Provision of the cohorts' clinical data as well as the gas exchange and therapy details for every patient. **Vincenzo L'Imperio:** Electron microscopy, supervision of the drafting of the manuscript, and critical revision of the final version of the manuscript. All the authors approved the submitted version of the manuscript.

REFERENCES

- Zhu N, Zhang D, Wang W, et al. A novel coronavirus from patients with pneumonia in China, 2019. *N Engl J Med.* 2020;382:727-733.
- Nicholson AG, Osborn M, Devaraj A, Wells AU. COVID-19 related lung pathology: old patterns in new clothing? *Histopathology.* 2020;77:169-172.
- Borczuk AC, Salvatore SP, Seshan SV, et al. COVID-19 pulmonary pathology: a multi-institutional autopsy cohort from Italy and New York City. *Mod Pathol.* 2020;33:2156-2168.
- Menter T, Haslbauer JD, Nienhold R, et al. Postmortem examination of COVID-19 patients reveals diffuse alveolar damage with severe capillary congestion and variegated findings in lungs and other organs suggesting vascular dysfunction. *Histopathology.* 2020;77:198-209.
- Giani M, Seminati D, Lucchini A, Foti G, Pagni F. Exuberant plasmocytosis in bronchoalveolar lavage specimen of the first patient requiring extracorporeal membrane oxygenation for SARS-CoV-2 in Europe. *J Thorac Oncol.* 2020;15:e65-e66.
- Liao M, Liu Y, Yuan J, et al. Single-cell landscape of bronchoalveolar immune cells in patients with COVID-19. *Nat Med.* 2020;26:842-844.
- Horby P, Lim WS, Emberson JR, et al; RECOVERY Collaborative Group. Dexamethasone in hospitalized patients with COVID-19—preliminary report. *N Engl J Med.* Published online July 17, 2020. doi:10.1056/NEJMoa2021436
- Lamontagne F, Agoritsas T, Macdonald H, et al. A living WHO guideline on drugs for COVID-19. *BMJ.* 2020;370:m3379.
- Lucchini A, Giani M, Winterton D, Foti G, Rona R. Procedures to minimize viral diffusion in the intensive care unit during the COVID-19 pandemic. *Intensive Crit Care Nurs.* 2020;60:102894.
- Barbareschi M, Ascoli V, Bonoldi E, et al. Biosafety in surgical pathology in the era of SARS-Cov2 pandemic. A statement of the Italian Society of Surgical Pathology and Cytology. *Pathologica.* 2020;112:59-63.

11. Centers for Disease Control and Prevention. Interim guidelines for collecting, handling, and testing clinical specimens for COVID-19. Accessed December 23, 2020. <https://www.cdc.gov/coronavirus/2019-nCoV/lab/guidelines-clinical-specimens.html>
12. Verga L, Leni D, Cazzaniga G, et al. The spectrum of the cytopathological features of primary effusion lymphoma and human herpes virus 8–related lymphoproliferative disorders. *Cytopathology*. 2020;31:541-546.
13. Mansy SS. Agarose cell block: innovated technique for the processing of urine cytology for electron microscopy examination. *Ultrastruct Pathol*. 2004;28:15-21.
14. Kamel T, Helms J, Janssen-Langenstein R, et al. Benefit-to-risk balance of bronchoalveolar lavage in the critically ill. A prospective, multicenter cohort study. *Intensive Care Med*. 2020;46:463-474.
15. Meyer KC, Raghu G, Baughman RP, et al. An official American Thoracic Society clinical practice guideline: the clinical utility of bronchoalveolar lavage cellular analysis in interstitial lung disease. *Am J Respir Crit Care Med*. 2012;185:1004-1014.
16. Bouros D, Nicholson AC, Polychronopoulos V, du Bois RM. Acute interstitial pneumonia. *Eur Respir J*. 2000;15:412-418.
17. Juss JK, House D, Amour A, et al. Acute respiratory distress syndrome neutrophils have a distinct phenotype and are resistant to phosphoinositide 3-kinase inhibition. *Am J Respir Crit Care Med*. 2016;194:961-973.
18. Potey PM, Rossi AG, Lucas CD, Dorward DA. Neutrophils in the initiation and resolution of acute pulmonary inflammation: understanding biological function and therapeutic potential. *J Pathol*. 2019;247:672-685.
19. Wang Y, Ju M, Chen C, et al. Neutrophil-to-lymphocyte ratio as a prognostic marker in acute respiratory distress syndrome patients: a retrospective study. *J Thorac Dis*. 2018;10:273-282.
20. Tate MD, Ioannidis LJ, Croker B, Brown LE, Brooks AG, Reading PC. The role of neutrophils during mild and severe influenza virus infections of mice. *PLoS One*. 2011;6:e17618.
21. Schutgens RE. D-dimer in COVID-19: a guide with pitfalls. *Hemasphere*. 2020;4:e422.
22. Padilla-Carlin DJ, Schladweiler MCJ, Shannahan JH, et al. Pulmonary inflammatory and fibrotic responses in Fischer 344 rats after intratracheal instillation exposure to Libby amphibole. *J Toxicol Environ Health A*. 2011;74:1111-1132.
23. Löffler C, Mahrhold J, Fogarassy P, Beyer M, Hellmich B. Two immunocompromised patients with diffuse alveolar hemorrhage as a complication of severe coronavirus disease 2019. *Chest*. 2020;158:e215-e219.
24. Bradley BT, Maioli H, Johnston R, et al. Histopathology and ultrastructural findings of fatal COVID-19 infections in Washington State: a case series. *Lancet*. 2020;396:320-332.
25. Carsana L, Sonzogni A, Nasr A, et al. Pulmonary post-mortem findings in a series of COVID-19 cases from northern Italy: a two-centre descriptive study. *Lancet Infect Dis*. 2020;20:1135-1140.
26. Stadlmann S, Hein-Kuhnt R, Singer G. Viropathic multinuclear syncytial giant cells in bronchial fluid from a patient with COVID-19. *J Clin Pathol*. 2020;73:607-608.
27. Grasselli G, Foti G, Patroniti N, et al. A case of ARDS associated with influenza A—H1N1 infection treated with extracorporeal respiratory support. *Minerva Anestesiol*. 2009;75:741-745.
28. Miller SE, Brealey JK. Visualization of putative coronavirus in kidney. *Kidney Int*. 2020;98:231-232.
29. Weinberg SE, Behdad A, Ji P. Atypical lymphocytes in peripheral blood of patients with COVID-19. *Br J Haematol*. 2020;190:36-39.
30. Tavakolpour S, Rakhshandehroo T, Wei EX, Rashidian M. Lymphopenia during the COVID-19 infection: what it shows and what can be learned. *Immunol Lett*. 2020;225:31-32.
31. Wu MY, Yao L, Wang Y, et al. Clinical evaluation of potential usefulness of serum lactate dehydrogenase (LDH) in 2019 novel coronavirus (COVID-19) pneumonia. *Respir Res*. 2020;21:171.